

Temperature and frequency dependences of the dielectric properties of $\text{YBa}_2\text{Cu}_3\text{O}_{6+x}$ ($x \approx 0$)

G. A. Samara, W. F. Hammetter, and E. L. Venturini

Sandia National Laboratories, P.O. Box 5800, Albuquerque, New Mexico 87185

(Received 29 June 1989; revised manuscript received 28 December 1989)

The real (ϵ') and imaginary (ϵ'') parts of the dielectric constant of dense tetragonal ceramic (91–93% of theoretical density) $\text{YBa}_2\text{Cu}_3\text{O}_{6+x}$ samples with $x = 0.04$ and 0.06 were investigated as functions of temperature (4–300 K) and frequency (10^2 – 10^6 Hz). At 4K the dielectric loss is very small ($\tan \delta < 0.005$) and $\epsilon' = 14.7 \pm 0.3$, independent of frequency. This value of ϵ' represents the intrinsic value of the static dielectric constant of the material, i.e., the combined electronic and lattice contributions to ϵ' . Both ϵ' and ϵ'' exhibit small increases with increasing temperature at low temperatures—behavior characteristic of normal dielectrics; however, on further heating strong increases and frequency dispersions develop. Above ~ 160 K, the $\epsilon'(T)$ and $\epsilon''(T)$ responses are nearly exponential. These temperature and frequency effects are interpreted in terms of dipolar polarization associated with the hopping motion of localized charge carriers. Consistent with this view, the observed frequency dependence of the conductivity is found to obey a power law of the form $\sigma(\omega) = A\omega^s$, where s is a temperature-dependent constant (< 1) and ω is the angular frequency. The results can be well represented by Pike's classical hopping model which yields explicitly the ω^s behavior, the temperature dependence of s , and the energy barrier to the hopping process.

I. INTRODUCTION

The discovery of high-temperature superconductivity (T_c above 90 K) in $\text{YBa}_2\text{Cu}_3\text{O}_{6+x}$, the so-called "1:2:3" material system, has generated great interest in the physical properties of these materials. A very intriguing property of this system is the ease by which oxygen can be taken up or removed from it, making it possible to vary x continuously from 0 to 1.^{1,2}

The system crystallizes in a layered perovskitelike structure, a key feature of which is the arrangement of the copper and the bridging oxygen ions.^{1–3} These ions lie in infinite layers, or sheets, with an ABC, ABC, \dots sequence. Layers A and C consist of CuO_2 units, whereas layer B has variable O content. For $x = 0$, the O sites in the B layer are empty, and the crystal structure is tetragonal ($P4/mmm$), the c axis being perpendicular to the layers. The addition of O causes random filling of the four equivalent sites between the Cu ions in the B layer, and the structure remains tetragonal up to $x = 0.4$. For $x > 0.4$, the O's tend to order into chains along one of the tetragonal a axes. This ordering breaks the tetragonal symmetry and the crystal structure becomes orthorhombic ($Pmmm$). At $x = 1$ half of the O sites in the B layer are filled forming complete Cu-O chains. In the tetragonal phase ($0 \leq x < 0.4$), the materials are insulating antiferromagnets, the magnetic Cu spins being aligned in the planes of the A and C layers. Superconductivity is observed only in the orthorhombic phase with T_c increasing from < 40 K to ~ 90 K as x increases from ≈ 0.4 to 1.0.¹

Although there appears to be no overlap between the insulating antiferromagnetic and superconducting phases, it is generally believed that understanding the behavior in the tetragonal insulating phase may shed some light on the mechanism of superconductivity in these materials.

This view has motivated studies of the electronic transport⁴ and magnetism³ of the insulating phase. The dielectric properties of this phase can also provide important insights; however, no systematic studies have been reported. It has been observed^{5–8} that several of the CuO_2 -based high- T_c materials, including tetragonal 1:2:3, have relatively large, temperature-dependent dielectric constants. Since such dielectric behavior is often the signature of ferroelectricity or incipient ferroelectricity in many perovskite oxides, it has been tempting to suggest the possibility of a common origin of ferroelectricity and high- T_c superconductivity in oxides. Bussmann-Holder *et al.*⁹ have recently drawn attention to this possibility and described a lattice dynamical model for displacive-type (or soft mode) ferroelectrics which might be applied to high-temperature superconductors. Dielectric constant results⁸ of Testardi *et al.* on a polycrystalline 1:2:3 sample quenched from high temperature (> 1170 K) as well as earlier results on $\text{BaBi}_{1-x}\text{Pb}_x\text{O}_3$ are cited by Bussmann-Holder *et al.* as providing possible confirmation of the competition between electron-electron pairing instability and ferroelectricity in this material. Kurtz *et al.*⁷ have also proposed that 1:2:3 and related materials may transform on cooling to a relaxor ferroelectric state prior to the onset of superconductivity.

Testardi *et al.*⁸ reported measurement of the dielectric constant of a highly porous (density $\approx 70\%$ of theoretical) polycrystalline sample of 1:2:3. The sample was prepared by quenching from $1170 \text{ K} < T < 1220 \text{ K}$. The oxygen content was not specified. The work is not detailed or complete in that only the real part of the dielectric constant (ϵ') at only one frequency (20 kHz) was reported with the indication that ϵ' increases nearly linearly with temperature from ~ 100 at 20 K to ~ 650 at 250 K. Below 20 K, ϵ' decreases sharply with decreasing T .

This temperature dependence is unusual for a dielectric or ferroelectric. Unfortunately, the complementary imaginary part of the dielectric constant, or the dielectric loss, was not reported.

The present work was motivated by the need for a detailed study of the dielectric properties of tetragonal insulating 1:2:3. In the absence of suitable single crystals, the measurements were made on two high-density ($\sim 91\text{--}93\%$ of theoretical) ceramic samples with $x=0.04$ and 0.06 . The results allowed evaluation of the real and imaginary parts of the dielectric constant from 4 to ~ 300 K and over the frequency range 10^2 to 10^6 Hz. In what follows, the experimental details are summarized, and this is followed by presentation and discussion of the results. It will be shown that the results do indeed provide important insights into the behavior of this material.

II. EXPERIMENTAL DETAILS

The real (ϵ') and imaginary (ϵ'') parts of the complex dielectric constant $\epsilon(=\epsilon'-i\epsilon'')$ of two polycrystalline, insulating 1:2:3 samples were determined from capacitance, dielectric loss ($\tan\delta$) and complex impedance measurements performed as functions of temperature (4– ~ 300 K) and frequency (10^2 – 10^6 Hz). The results represent polycrystalline averages of the anisotropic (tetragonal a and c axes) values of these properties.

The samples were made by mixing stoichiometric proportions of reagent grade Y_2O_3 , $Ba(NO_3)_2$, and CuO in a polyethylene jar with methanol and Al_2O_3 milling media for 16 h. The mixture was first dried then calcined in air at 925°C for 4 h. The resulting porous compact was ground by hand and screened to -200 mesh. That powder was uniaxially pressed at 34.5 MPa (5000 psi) into bars approximately $5.08 \times 0.64 \times 0.64$ cm³ which were then isostatically pressed at 172.4 MPa (25000 psi.). The bars were sintered at 950°C for 4 h in air; thereafter the atmosphere was switched to oxygen and the temperature lowered to 900°C for another 4 h soak. From 900°C the samples were cooled slowly ($5^\circ\text{C}/\text{h}$) to 480°C and held for 14 h. The samples were then furnace cooled to room temperature under oxygen. Sample densities were typically $91\text{--}93\%$ of theoretical and contained $6.89\text{--}6.91$ oxygens per formula unit as measured by reduction to the oxides (and Cu metal) in hydrogen.¹⁰

To establish the quality of the starting samples for the present work, the superconducting properties of thin plates cut from an as-prepared $YBa_2Cu_3O_{6+x}$ bar were determined by static magnetization measurements in a commercial SQUID susceptometer. Flux exclusion (diamagnetic shielding) and flux expulsion (Meissner effect) were measured versus magnetic field and temperature for plates approximately $6.6 \times 5.3 \times 0.6$ mm³; the field was applied parallel to the long dimension to minimize demagnetization effects. One such plate weighed 140.5 mg, corresponding to a density of 91% of the theoretical value of 6.36 g/cm³. The shielding response versus increasing field at 5 K following zero-field cooling showed the well-documented grain decoupling¹¹ near 2.5 mT. At lower fields the volume susceptibility $\chi_v = -1.02/4\pi$, corresponding to complete flux exclusion ($-1/4\pi$) with

a 2% enhancement due to the very small demagnetization. Above 5 mT the shielding response was also linear in applied field with $\chi_v = -0.83/4\pi$; half of the reduction below complete exclusion is attributed to the grain decoupling which exposes the pores of the ceramic to field penetration, while the remainder is largely due to the field penetration depth (≈ 1500 Å) into the individual grains. Except for the grain decoupling, the large shielding response suggests high-quality ceramic $YBa_2Cu_3O_{6+x}$.

Figure 1 shows flux exclusion (solid circles) versus increasing temperature and flux expulsion (open triangles) versus decreasing temperature between 5 and 100 K in a field of 2.5 mT applied parallel to a cut plate. The sharp onset of superconductivity near 93 K, the rapid rise in both exclusion and expulsion, and the nearly flat response below liquid nitrogen temperature all attest to the homogeneity of the superconducting $YBa_2Cu_3O_{6+x}$ grains, both in cation stoichiometry and oxygen concentration. The factor of three difference in exclusion and expulsion at low temperature is attributed to flux pinning which occurs both at grain and twin boundaries in this orthorhombic material. Again, the data in Fig. 1 are the best observed to date in ceramic $YBa_2Cu_3O_{6+x}$, and are consistent with high-quality material.

Having established the high quality of the starting samples, slabs of approximately $9 \times 7 \times 0.7$ mm³ were cut from the as-prepared bars. The oxygen contents of the slabs were normalized by heating in oxygen to 1170 K at 2 K/min, holding for one hour and then cooling to room temperature at 0.5 K/min. Based on our past results¹² we believe this treatment fixes the oxygen content at about 6.90 oxygens per formula unit. Two of the normalized slabs were then heated to 1100 K in 1000 ppm O_2/Ar and held for 30 min. The atmosphere was then purged with pure argon for 10 min after which time the slabs were quenched to room temperature. The weight changes show the oxygen contents to be 6.04 and 6.06 oxygen atoms per formula unit. X-ray diffraction measure-

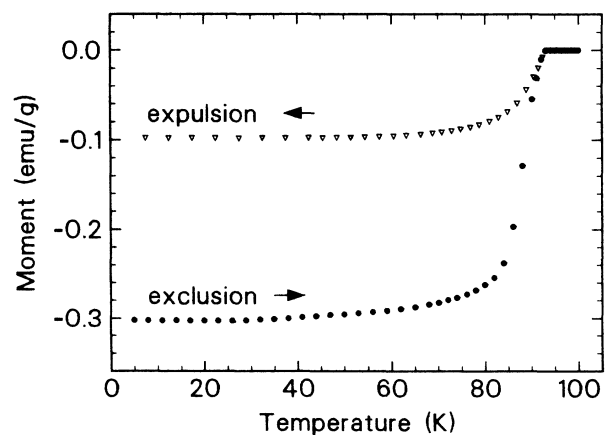


FIG. 1. Flux exclusion (solid circles) vs increasing temperature and flux expulsion (open triangles) vs decreasing temperature for a cut thin plate of ceramic $YBa_2Cu_3O_{6+x}$ ($x \approx 0.90$) oriented parallel to a 2.5 mT applied field.

ments showed the samples to be in the tetragonal phase, and the densities were $\sim 92\%$ of the theoretical. The room-temperature resistivities were 250–270 Ω cm.

Within a few hours after quenching, the large surfaces of the samples were dry polished and electroded with air-drying silver paint. These electrodes adhered well and gave reversible, reproducible results. In measurements on insulating La_2CuO_4 we found that these electrodes and sputtered gold electrodes gave identical results. When not in use the samples were always kept in a dry atmosphere in a desiccator. The dielectric measurements were started within a few days after quenching and electroding. The reproducibility and reversibility of the data over the course of the experiments (many days) showed that there were no aging effects.

The details of the experiments were similar to those reported earlier.¹³ The capacitance, dissipation, and complex impedance of the samples were measured using Hewlett-Packard instruments—an LCR bridge model 4275A and an impedance bridge model 4192A. The temperature measurements were performed with the sample mounted in a helium gas-filled cell placed inside a conventional low-temperature Dewar. Temperature changes were measured to better than ± 0.1 K using Cu-constantan and Au-Au Fe thermocouples. The experimental setup made it most convenient to take data on the warm-up cycle. Consequently, all the data presented were obtained on warming up the samples from 4 K. However, data were also obtained on cooling at a fixed temperature (76 K) and were in good agreement with the data obtained on warming. ϵ' and ϵ'' were calculated from the measured capacitances (or impedances) without correction for changes in sample dimensions due to thermal expansion. Such changes are usually small¹³ and are of no consequences for the present purposes.

III. RESULTS AND DISCUSSION

Measurements on single crystals of orthorhombic superconducting 1:2:3 revealed significant anisotropy in the electronic properties as functions of crystallographic orientation.¹⁴ It is reasonable to expect some anisotropy in the electronic and dielectric properties of the tetragonal insulating phase as well. Although the present measurements were performed on high-quality, dense ceramic samples, it should be emphasized that the reported dielectric constants represent polycrystalline averages.

The results on the $x=0.04$ and 0.06 samples were qualitatively, and in most important respects, quantitatively similar. All the data were reproducible and reversible on temperature cycling. This was not the case in earlier attempts at the same measurements using normally sintered low-density ceramics.

The main results are summarized in Figs. 2–4. Figure 2 shows the $\epsilon'(T)$ and $\epsilon''(T)$ results at different frequencies (f) for the $x=0.06$ sample. Figure 3 provides, on an expanded scale, a more detailed view of the temperature and frequency dependences of the dielectric loss, $\tan\delta(=\epsilon''/\epsilon')$, for the same sample. For comparison, Fig. 4 presents results for the $x=0.04$ sample. Here we emphasize the low-temperature (< 80 K) responses.

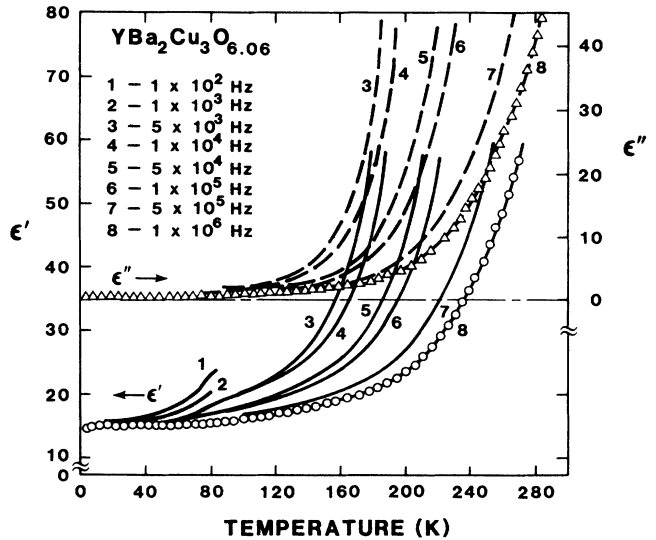


FIG. 2. Temperature dependence of the real (ϵ') and imaginary (ϵ'') parts of the dielectric constant of dense ceramic $\text{YBa}_2\text{Cu}_3\text{O}_{6.06}$ at different frequencies.

Above 80 K the responses are qualitatively similar to those of the $x=0.06$ sample. We note that these responses are qualitatively and quantitatively different from that reported by Testardi *et al.*⁸

Three general features of the results in Figs. 2–4 are noteworthy. First, we note that at the lowest temperatures both ϵ' and ϵ'' become frequency and very nearly temperature independent. At 4 K, $\tan\delta < 0.005$, implying that both samples are good, low loss, dielectrics, and ϵ' reaches a limiting value of 14.7 ± 0.3 . Note that both ϵ' and ϵ'' approach their 4 K values from higher temperatures with zero slope, i.e., $d\epsilon'/dT$ and $d\epsilon''/dT \rightarrow 0$ K, as is expected on thermodynamic grounds. Second, both ϵ' and ϵ'' increase with increasing T , and strong frequency dispersions develop as shown. Above ~ 160 K, the $\epsilon'(T)$ and $\epsilon''(T)$ responses are nearly exponential. Third, the results reveal shoulders in the $\epsilon(T, f)$ responses in the re-

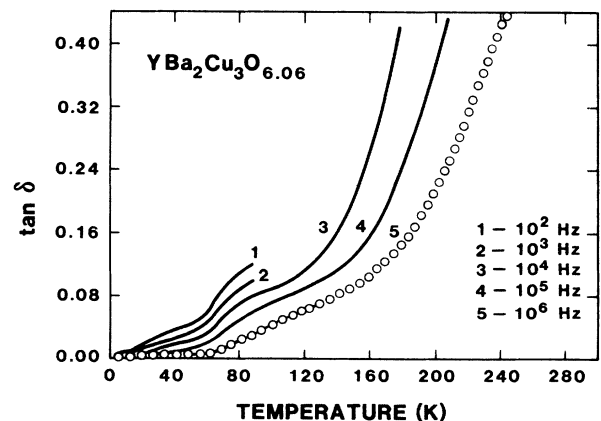


FIG. 3. Temperature dependence of the dielectric loss, $\tan\delta$, of dense ceramic $\text{YBa}_2\text{Cu}_3\text{O}_{6.06}$ at different frequencies.

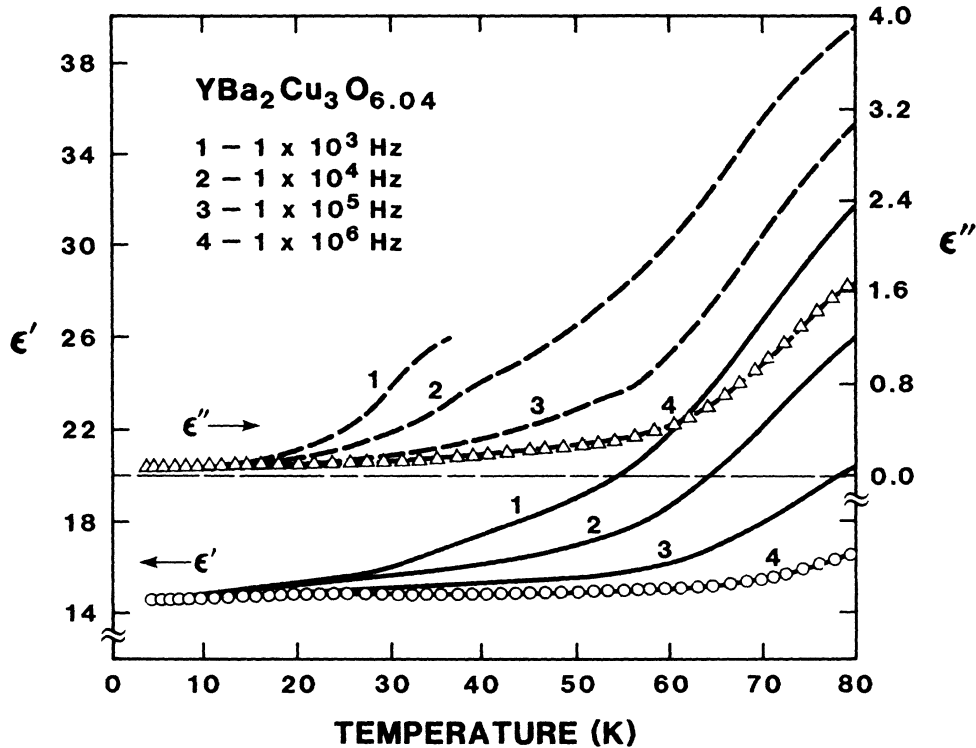


FIG. 4. Temperature dependence of the real (ϵ') and imaginary (ϵ'') parts of the dielectric constant of dense ceramic $\text{YBa}_2\text{Cu}_3\text{O}_{6.04}$ at different frequencies.

gions 30–40 K and 60–80 K. These shoulders, which are most clearly seen in the expanded data in Fig. 3, could be due to the presence of some minority phases or impurities in the samples. It is known¹ that there is a second superconducting “phase” with $T_c \approx 60$ K in orthorhombic 123, and it is likely that some manifestation of this phase survives in the tetragonal phase. We now wish to discuss the first two features.

The complex dielectric function, $\epsilon = \epsilon' - i\epsilon''$, which describes the response of a solid to an oscillating electric field, is generally determined by three sources of polarization and can be written as

$$\epsilon = \epsilon_\infty + \epsilon_l + \epsilon_d. \quad (1)$$

The first contribution, ϵ_∞ , is the electronic, or high-frequency dielectric constant which arises from the polarization associated with the displacements of the electronic charge distributions of the atoms or ions relative to their nuclei. The second, or lattice, contribution ϵ_l , arises from the polarization associated with the combined effects of the displacement of the ions and the accompanying displacements of the electronic charge distributions. The third contribution, ϵ_d , arises from dipolar polarization associated with the presence of either permanent orientable dipoles (not present in the 1:2:3 materials) or dipolar effects produced by impurities, lattice defects, or the presence of charge carriers. These three contributions are not completely independent: however, they exhibit different frequency responses and can thus be separated. At very low frequencies, all three sources of

polarization are important, whereas at optical frequencies, i.e., above optical phonon frequencies, only the electronic polarization comes into play. In the absence of dipolar polarization, ϵ should be nondispersive for frequencies up to microwave frequencies. Thus, dispersion below microwave frequencies results from dipolar polarization effects. These effects are known to exhibit a variety of characteristic frequency and temperature responses.¹⁵

The fact that ϵ' and ϵ'' become independent of frequency at the lowest temperatures in Figs. 2 and 4 indicates that the observed response represents the true static dielectric response of this ceramic 1:2:3 material in the absence of dipolar effects. The observed value of ϵ' at 4 K is the same (14.7 ± 0.3) for both samples and represents essentially $\epsilon'_\infty + \epsilon'_l$ for this material. Although the data show that a strong frequency dispersion in both ϵ' and ϵ'' develops with increasing T , this dispersion vanishes for $f \geq 5 \times 10^5$ Hz below ~ 60 K. Thus, the $\epsilon'(T)$ response between 4 and 60 K at 10^6 Hz in Figs. 2 and 4 reflects the temperature dependence of $(\epsilon'_\infty + \epsilon'_l)$. We note that in this regime, ϵ' increases slightly with increasing temperature, behavior characteristic of normal dielectrics.¹⁶ This increase, which is shown more clearly for the $x=0.04$ sample at 10^6 Hz in Fig. 4, results primarily from the increase in lattice polarizability, or softening of the lattice, with increasing T .

The relatively large increases in the magnitudes of, and the strong frequency dispersion in, both ϵ' and ϵ'' observed at the higher temperatures in Figs. 2–4 are characteristic of dipolar effects which are controlled by the activation of defects and/or localized charge centers.

Localized charge carriers are believed to be prevalent in the insulating phase of the CuO_2 -based oxides,¹⁷ and charge transport presumably occurs by hopping motion. Under ac field excitation, hopping, or oscillatory, motion of carriers leads to a net polarization or current. The in-phase (with the field) component of the polarization is responsible for the dipolar contribution to the real part of ϵ' , i.e., ϵ'_d , whereas the out-of-phase component is reflected in the dipolar part of the dielectric loss $\tan\delta$ (or ϵ''_d). The dielectric loss is related to the dipolar conductivity, σ_d by the expression

$$\tan\delta = \epsilon''_d / \epsilon'_d = 4\pi\sigma_d / \epsilon'_d\omega, \quad (2)$$

where $\omega (= 2\pi f)$ is the angular frequency.

For many crystalline and noncrystalline solids known to exhibit hopping electronic transport, the frequency dependence of σ_d is known to obey a power law of the form¹⁸⁻²¹

$$\sigma_d(\omega) = A_1\omega^s \quad (3a)$$

$$= \omega\epsilon''_d(\omega) / 4\pi, \quad (3b)$$

where A_1 generally exhibits a weak T dependence, $s \leq 1$ and Eq. (3b) follows from Eq. (2). The real part of the polarization, or ϵ'_d , also has a characteristic frequency response; however, the two responses are not independent of each other but, rather, are related by the Kramers-Kronig relations. Specifically, given Eq. (3), it can be shown²² that the Kramers-Kronig relations lead to

$$\omega\epsilon'_d(\omega) = A_2\omega^s \quad (4a)$$

$$= \sigma_d(\omega)\tan(s\pi/2), \quad (4b)$$

where $A_2 = A_1\tan(s\pi/2)$.

We will now show that the present data are well represented by Eqs. 3 and 4. Some results are shown in Fig. 5. Plotted are $\log(\omega\epsilon'_d)$ vs $\log f$ at constant $T=160$ K. The symbols represent the data determined directly from the measurements. It is seen that such plots are linear over the ranges covered, and in both cases the exponent $s = 0.69 \pm 0.01$. The applicability of the Kramers-Kronig relations is demonstrated by the dashed line in Fig. 5. This dashed line, which represents $\omega\epsilon'_d(\omega)$ calculated from Eq. (4b), provides an excellent fit to the directly measured $\omega\epsilon'_d(\omega)$ data represented by the triangles.

As is commonly observed in systems exhibiting hopping electronic transport,¹⁸⁻²¹ we find the exponent s exhibits significant temperature dependence. Specifically, for the $x=0.06$ sample, $s = 1.0, 0.80, 0.69,$ and $0.60,$ at $4, 80$ K, 160 K, and 190 K, respectively. Similar results were obtained for the $x=0.04$ sample. We shall discuss this temperature dependence of s below.

Turning next to the temperature dependence, Fig. 6 shows $\log\epsilon''$ versus T^{-1} plots at fixed frequencies. At high temperatures, the $\epsilon''(T)$ response becomes fairly well describable by the simple Arrhenius equation

$$\epsilon'' \propto \exp(-E/kT). \quad (5)$$

This can be seen to be the case for the 10^4 Hz data for

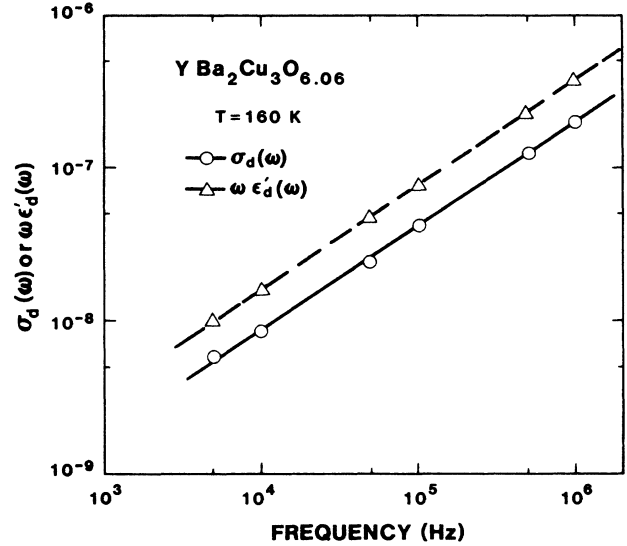


FIG. 5. Power-law dependence on frequency of the real (σ_d) and imaginary ($\omega\epsilon'_d$) parts of the complex dipolar, or polarization, conductivity of $\text{YBa}_2\text{Cu}_3\text{O}_{6.06}$. The dashed line is the theoretical result for $\omega\epsilon'_d$ calculated from σ_d using Eq. (4b).

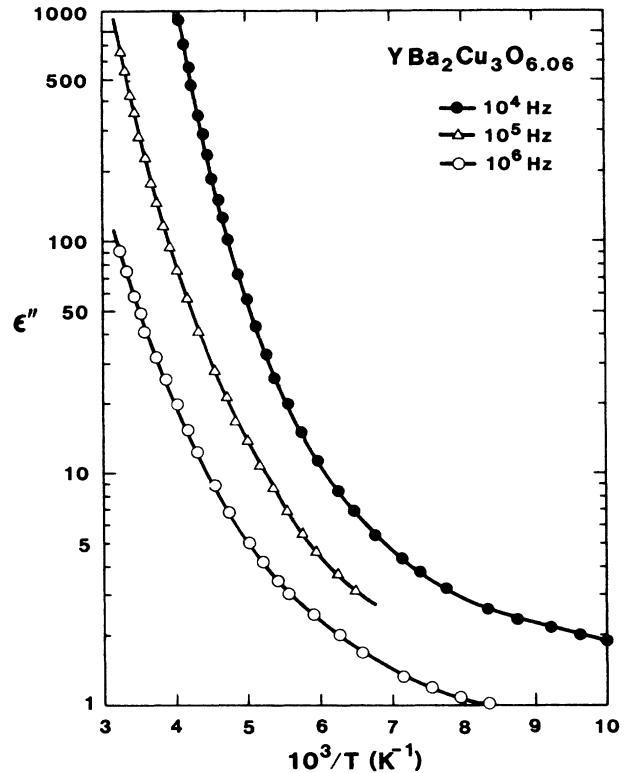


FIG. 6. Temperature dependence of the imaginary part of the dielectric constant ($\epsilon'' \propto \sigma_d$) of $\text{YBa}_2\text{Cu}_3\text{O}_{6.06}$ measured at different frequencies.

$T > 200$ K, where $E = 0.28$ eV. This high- T regime is attained at higher temperatures the higher the frequency. At lower T 's, the response becomes non-Arrhenius with the slope in Fig. 6 (or E) decreasing continuously with decreasing T .

The observed non-Arrhenius behavior of $\epsilon''(T)$ in Fig. 6 is characteristic of certain models of hopping transport. Such behavior is predicted, for example, from Emin's theoretical studies²³ of phonon-assisted hopping. Specifically, it is argued that the large decrease in E with decreasing T for intrinsic hopping is due to the freezing out of phonon-assisted hopping processes, it being a fact that the number of available phonons decreases with decreasing T . In this model, at sufficiently high T 's, multiphonon processes become prevalent, and the temperature dependence of the conductivity [or more appropriately, the mobility, μ , since $\sigma(T)$ is determined by $\mu(T)$] becomes essentially Arrhenius. Specifically, in this high- T regime, μ is given by²³

$$\mu \propto T^{-1} \exp(-E'/kT). \quad (6)$$

As already noted, above 200 K the 10^4 Hz data in Fig. 6 can be well described by Eq. (5). However, we note here that over the limited temperature range covered, the data can be equally well fit by the expression $\epsilon'' \propto T^{-1} \exp(-E'/kT)$ as dictated by Eq. (6). Thus, the data are consistent with the high- T limit of the phonon-assisted hopping model. The transition from the high- T to the low- T regime (i.e., change in slope in Fig. 6) is predicted²³ to occur at $\sim \frac{1}{3}$ the Debye temperature, Θ_D . This behavior has been confirmed for some materials, e.g., the hopping transport of holes in amorphous silica (SiO_2).²⁴ For the Cu_2O -based high- T_c oxides, Θ_D is expected to be in the range 500–600 K, so that the crossover from high- T to low- T behavior is consistent with the model.

To pursue the frequency and non-Arrhenius temperature dependences of ϵ'' further, we resort to Pike's model²⁰ of hopping transport which yields explicitly the ω^s behavior, the temperature dependence of s and the energy barrier to the hopping process. In this model, transport occurs by hopping over potential barriers separating localized sites. The model is depicted in Fig. 7 which

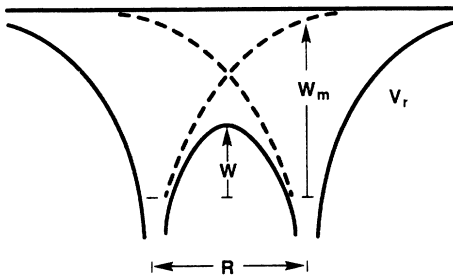


FIG. 7. Model of overlapping Coulomb-like potentials V_r (after Pike, Ref. 20). The potentials are centered a distance R apart. The ground state (ionization) energy is W_m , and the potential barrier between the two localized states is W . Note that W is a strong function of R .

shows two localized sites separated by a distance R . The problem is treated in the classical limit in which carrier motion is characterized by an activation energy, W , which is calculated for a specific form of the site potential (taken to be Coulomb-like in Fig. 7). The barrier height W is related to R which is determined by a random spatial distribution of the localized sites. W_m in Fig. 7 is the energy difference between the ground state of the potential well and the ionized (band or extended) state. At low temperatures, sites with small separations, or small W [and hence small E in Eqs. (5) and (6)] are dominant, whereas with increasing T longer hops, or larger W 's, become important. This provides a natural explanation for the observed increase of E with increasing T in Fig. 6. At low to modest temperatures, the model yields

$$1-s = 6kT/W_m, \quad (7)$$

so that the quantity $(1-s)$ is predicted to vary linearly with T with a slope inversely proportional to W_m . Figure 8 shows that our data for 1:2:3 follow this prediction. From the slope in Fig. 8 we calculate $W_m = 0.26$ eV which is in rather good agreement with the value of $E = 0.28$ eV deduced directly from the 10^4 Hz data for $T > 200$ K in Fig. 6. It is thus seen that the present data can be remarkably well represented by Pike's model.²⁰

Pike's model is one variant of variable range hopping. An alternative model for the non-Arrhenius behavior of $\epsilon''(T)$ is Mott's original variable-range hopping model.²⁵ Here the continuous decrease in E with decreasing T is presumed to be due to the increase in average hopping distance (or decrease in hopping rate) at low T 's as the carriers sample more distant sites that are more closely matched in energy. According to this mode, σ , at low temperatures is given by

$$\sigma \propto A \exp(-B/T^{1/x}), \quad (8)$$

where $x=4$ for a three-dimensional system and $x=3$ for a two-dimensional system. Results on the T dependence of the resistivity of single crystal La_2CuO_4 below ~ 100 K have been interpreted in terms of Eq. (7). Kastner *et al.*^{17(a)} find $x=4$, whereas Oda *et al.*^{17(b)} find $x=3$ which is characteristic of 2D transport, and the latter authors argue that this behavior is consistent with the an-

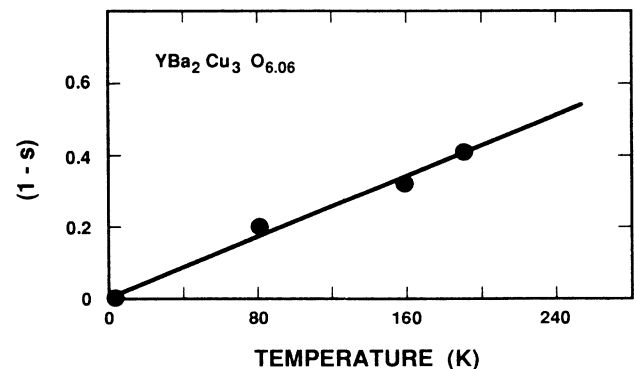


FIG. 8. Temperature dependence of the exponent s in the power law $\sigma_d \propto \omega^s$ (expressed as $1-s$) for $\text{YBa}_2\text{Cu}_3\text{O}_{6.06}$.

isotropic nature of the transport in La_2CuO_4 .

In order to test the viability of Eq. (8) $\sigma(T)$ data are needed over a broad range of T . In most reported cases, the $(1/T^{1/x})$ regime extends over a relatively narrow T range making it difficult to definitively establish this T dependence. For the present 1:2:3 material, the data between 100 and 200 K in Fig. 5 do not cover a sufficiently broad T range, and the data below 100 K are, unfortunately, complicated by the aforementioned shoulders in the $\epsilon''(T)$ response in the regions 30–40 K and 60–80 K (see Figs. 1–3), making it difficult to test the applicability of Eq. (8) in this region.

IV. CONCLUDING REMARKS

In this paper we have presented and discussed the effects of temperature (4–300 K) and frequency (10^2 – 10^6 Hz) on the real (ϵ') and imaginary (ϵ'') parts of the dielectric constant of $\text{YBa}_2\text{Cu}_3\text{O}_{6+x}$ in the ultimate insulating limit of $x \approx 0$. For high-quality ceramic samples (91–93 % of theoretical density) with $x = 0.04$ and 0.06 , the static dielectric constant, ϵ' , is found to be 14.7 ± 0.3 at 4 K, independent of frequency, and increases slightly with increasing temperature up to ~ 60 K—behavior characteristic of normal dielectrics. Relatively large increases in the magnitudes of, and strong frequency

dispersion in, both ϵ' and ϵ'' are observed at higher temperatures. These temperature and frequency effects are interpreted in terms of dipolar polarization associated with the hopping motion of localized charge centers. The results are found to be consistent with Pike's model²⁰ of classical hopping transport which is a variable-range hopping model.

An interesting and potentially significant question centers around the influence of the oxygen content, x , in the 1:2:3 material on the dielectric properties of the insulating phase ($0 \leq x \leq 0.40$). This question may be particularly important on approaching the onset of superconductivity at $x \approx 0.4$, since it may shed some light on the issues mentioned in the Introduction relating to the possibility of a connection between high- T_c superconductivity and ferroelectricity. Experiments on samples with different known oxygen contents are planned.

ACKNOWLEDGMENTS

We wish to express our thanks to L. V. Hansen and E. J. Binasiwicz for their expert technical assistance and to Dr. G. E. Pike for valuable technical discussion. The work performed at Sandia National Laboratories was supported by the U.S. Department of Energy under Contract No. DE-AC04-76-DP00789.

- ¹R. J. Cava, B. Battlogg, C. H. Chen, E. A. Rietman, S. M. Zahurak, and D. Werder, *Phys. Rev. B* **36**, 5719 (1987), and references therein.
- ²J. D. Jorgensen, B. W. Veal, W. K. Kwok, G. W. Crabtree, A. Umezawa, L. J. Nowicki, and A. P. Paulikas, *Phys. Rev. B* **36**, 5731 (1987), and references therein.
- ³J. M. Tranquada *et al.*, *Phys. Rev. B* **38**, 2477 (1988).
- ⁴See, e.g., W. K. Kwok *et al.*, *Phys. Rev. B* **37**, 106 (1988); Y. Mei *et al.*, *Z. Phys. B* **69**, 11 (1987).
- ⁵D. Reagor *et al.*, *Phys. Rev. Lett.* **62**, 2048 (1989).
- ⁶D. Emin and M. S. Hillery, *Phys. Rev. B* **39**, 6575 (1989).
- ⁷S. K. Kurtz *et al.*, *Mater. Lett.* **6**, 317 (1988); *Ferroelectrics* **87**, 29 (1988).
- ⁸L. R. Testardi *et al.*, *Phys. Rev. B* **37**, 2324 (1988).
- ⁹A. Bussmann-Holder, A. Simon, and H. Buttner, *Phys. Rev. B* **39**, 207 (1989).
- ¹⁰P. K. Gallagher *et al.*, *Mater. Res. Bull.* **22**, 995 (1987).
- ¹¹J. F. Kwak, E. L. Venturini, D. S. Ginley, and W. Fu, in *Novel Superconductivity*, edited by S. A. Wolf and V. Z. Kresin (Plenum, New York, 1987), pp. 983–991.
- ¹²W. F. Hammetter and E. J. Binasiwicz (unpublished).
- ¹³G. A. Samara, *Phys. Rev.* **165**, 959 (1968); *Phys. Rev. B* **13**, 4529 (1976).

- 4529 (1976).
- ¹⁴T. R. Dinger, T. K. Worthington, W. J. Gallagher, and R. L. Sandstrom, *Phys. Rev. Lett.* **58**, 2687 (1987).
- ¹⁵See, e.g., N. Hill *et al.*, *Dielectric Properties and Molecular Behavior* (Van Nostrand Reinhold, London, 1969). See also H. Frohlich, *Theory of Dielectrics* (Oxford University Press, Oxford, 1958).
- ¹⁶G. A. Samara, *Phys. Rev. B* **13**, 4529 (1976).
- ¹⁷(a) M. A. Kastner *et al.*, *Phys. Rev. B* **37**, 111 (1988); (b) M. Oda *et al.*, *Solid State Commun.* **67**, 257 (1988).
- ¹⁸N. F. Mott and E. A. Davis, *Electronic Processes in Noncrystalline Materials*, Second Edition (Clarendon, Oxford, 1979), p. 59.
- ¹⁹See, e.g., S. Golin, *Phys. Rev.* **132**, 178 (1963).
- ²⁰G. E. Pike, *Phys. Rev. B* **6**, 1572 (1972).
- ²¹M. Pollak and T. H. Geballe, *Phys. Rev.* **122**, 1742 (1961).
- ²²See, e.g., H. W. Bode, *Network Analysis and Feedback Amplifier Design* (Van Nostrand, Princeton, NJ, 1945), p. 314.
- ²³D. Emin, in *Physics of Structurally Disordered Solids* (1976), edited by S. S. Mitra (Plenum, New York, 1976), p. 461.
- ²⁴R. C. Hughes, *Phys. Rev. B* **15**, 2012 (1977).
- ²⁵See Ref. 17, p. 32 ff.